Real-Time Reactive Power Compensation of Induction Motor Loads Using Distribution-level Static Synchronous Compensator

Wei-Neng Chang, and Ching-Huan Liao

***Abstract*—**Real-time and continuous compensations of reactive power for induction motor loads in an industrial power system are very important, which not only can keep load bus voltage at a rated operation voltage, but also minimize the needed current for operations of induction motors. In the paper, a 7-level cascade full h-bridge converter based distribution-level static synchronous compensator (DSTATCOM) is developed for the real-time reactive power compensation and stability enhancement of induction motor loads in industrial power systems. First, the main circuit configuration and operation principle of the DSTATCOM are briefed. Then, a real-time reactive power compensation scheme is proposed for the DSTATCOM to continuously supply reactive power for the induction motor loads during transient starting and steady-state operation. Computer simulation is performed for preliminary verification. Finally, a DSTATCOM hardware prototype is built by using multi-DSP-based controller. Experimental results verify that the DSTATCOM can offer the real-time reactive power demand of the induction motor during free acceleration. The load bus voltage can also be stabilized to keep a good voltage regulation.

***Keywords*—**DSTATCOM, Induction motor loads, Hardware Implementation, Stability Enhancement.

I. Introduction

Induction motors are widely used in industries for a variety of loads, such as pumps, fans, compressors, valves, and conveyers. Starting of induction motor absorbing a large amount of reactive power produces voltage drop and disturbs sensitive loads connected in the same system. Steady-state operation of induction motor also needs reactive power, which causes poor load power factor and voltage regulation problem. Furthermore, induction motors are vulnerable to power system disturbance such as voltage sags caused by short-circuit faults [1-3]. Hence, real-time reactive power compensation of induction motor load is important for high quality power system operation in an industrial power system.

Traditionally, static var compensators (SVCs) are widely used for reactive power compensations and performance enhancements in industrial power systems [4-8]. However, the line-communication characteristic of the thyrisor-controlled-reactor (TCR) in the SVC limits the overall response time of the SVC [9-10]. Recently, due to rapid development of high power switching elements such as IGBTs and IGCTs, distribution-level static synchronous compensators (DSTATCOMs) have been recognized as the next-generation compensator for enhancement of power system performance [11-13]. Like a traditional SVC, DSTATCOM can be used for power factor correction, unbalanced load compensation, voltage flicker mitigation, and enhancement of system stability. Hence, The DSTATCOM is suitable for real-time reactive power compensation of induction motor loads in industries. Many types of converter configurations are used to construct the DSTATCOM main circuit, such as two-level, three-level, and multi-level converters. Among them, the multi-level cascade full h-bridge (FHB) converter based DSTATCOM has modular structure and better voltage stress withstand ability, which is more suitable for high power applications in the industries with induction motor loads [14-17].

A DSTATCOM with multilevel FHB converter for real-time reactive power compensation and performance enhancement of induction motor loads is proposed in the paper. The system architecture of the studied system is briefed in Sec. II. A real-time reactive power compensation scheme is developed in Sec. III for the DSTATCOM to continuously compensate the reactive power demand of induction motor loads. Sec. IV shows the simulation result for preliminary verification of the DSTATCOM. The hardware prototype of the DSTATCOM is built in Sec. V. Experimental results verify the effectiveness of the proposed DSTATCOM. Finally, Sec. VI gives the conclusion.

II. System Architecture

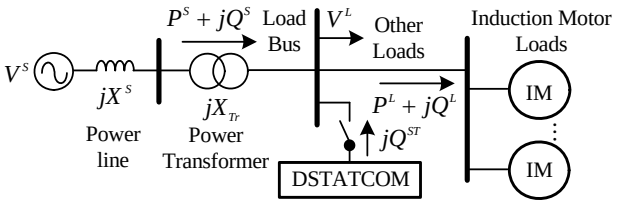

Fig. 1. An industrial power system with induction motor loads and the proposed DSTATCOM

W. N. Chang is with the Department of Electrical Engineering, Chang Gung University, 259 Wen-Hwa 1st Road, Kwei-Shan, Tao-Yuan,Taiwan (e-mail: nchang@mail.cgu.edu.com).

C. H. Liao is with the Department of Electrical Engineering, Chang Gung University, 259 Wen-Hwa 1st Road, Kwei-Shan, Tao-Yuan,Taiwan (e-mail: howardliao05@gmail.com).

Figure 1 shows an industrial power system with induction motor (IM) loads and the proposed DSTATCOM. The transient starting and steady-state operation of the induction motor loads in the manufacturing process need reactive power. The voltage drop on the load bus is expressed by (1). The load reactive power demand from the power source ($Q^S = Q^L$) produces undesired voltage drop.

$$\Delta V = Q^S (X^S + X_{Tr}) \tag{1}$$

The real-time reactive power compensation from the DSTATCOM locally supplies reactive power for the operations of the induction motor loads ($Q^S = Q^{ST} + Q^L = 0$). In this way, the reactive power from the power source is fully compensated to zero. This stabilizes the load bus voltage and corrects the load power factor to unity at the same time.

Figure 2 shows the proposed DSTATCOM main circuit with 7-level cascade FHB converter. A delta-connected configuration is used for the DSTATCOM main circuit [18-19]. The on-site reactive power compensation for the induction motor load is executed by the DSTATCOM.

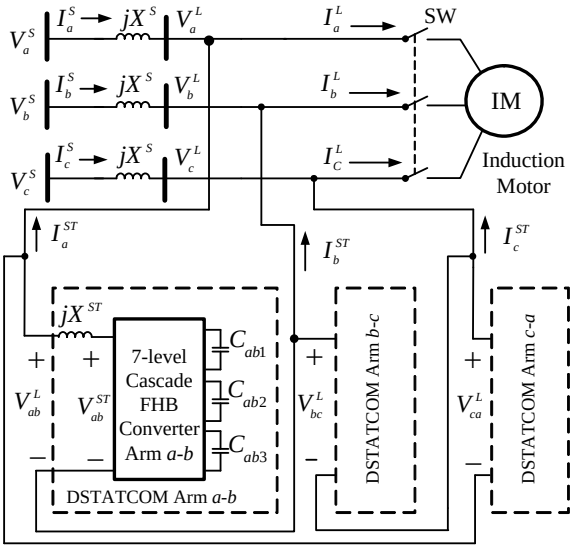

Fig. 2. The proposed DSTATCOM main circuit

Figure 3 shows the arm *a-b* structure of the DSTATCOM in Fig. 2. With proper control of gating signals, the DSTATCOM offers needed reactive power for the induction motor load. The DSTATCOM can be equivalent as a current-controlled source or voltage-controlled source. In the paper, the DSTATCOM is treated as a reactive power source.

The active power and reactive power outputs of each DSTATCOM arm are expressed by (2)-(3), respectively.

$$P^{ST} = \frac{V^{ST} V^L}{X^{ST}} \sin \delta^{ST} \tag{2}$$

$$Q^{ST} = \frac{V^L (V^{ST} \cos \delta^{ST} - V^L)}{X^{ST}} \tag{3}$$

An indirect control scheme is employed in the DSTATCOM for the reactive power control. For inductive load compensation, the DSTATCOM controller regulates the power angle δ^{ST} to a negative value. The DSTATCOM then absorbs active power from the power source according to (2). The active power input charges the dc-link capacitors in the FHB converters. The dc-link voltages are then boosted equally. The synthesized internal voltage V^{ST} of the DSTATCOM rises too. As a result, the DSTATCOM offers inductive reactive power like a capacitor bank according to (3) for the inductive load. Fig. 4 shows each level and internal voltage waveform of the DSTATCOM arm in Fig. 3, in which step modulation is used for high efficiency operation. The switching angles θ_1, θ_2, and θ_3 in Fig. 4 should be selected carefully for minimizing the undesired harmonic components [20-21].

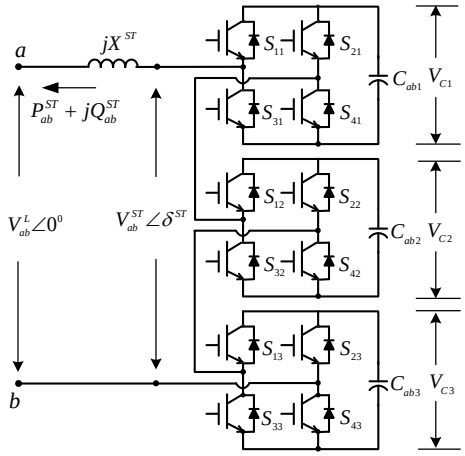

Fig. 3. Arm *a-b* structure of the DSTATCOM

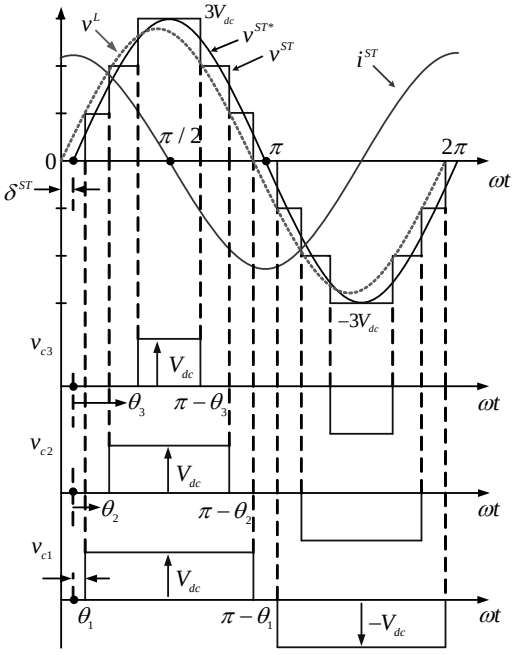

Fig. 4. Voltage and current waveforms of DSTATCOM arm

The internal voltage waveform v^{ST} in Fig. 4 can be represented as a Fourier series, as shown in (4). In (4), n is the harmonic order of the v^{ST}, where $n = 1,3,5,7,\ldots$. Ideally, the harmonic orders contain only odd orders without even order harmonic component. The amplitude of each harmonic component in (4) can further be represented in (5). Assigning $H(1) = 3V^{DC}$ for the fundamental compensation modulation and $H(5)=H(7)=0$ for the harmonic cancellation of the 5th and 7th orders obtain (5).

$$v^{ST}(\omega t) = \frac{4V^{DC}}{\pi}\sum_{n}\left[\cos(n\theta_1)+\cos(n\theta_2)+\cos(n\theta_3)\right]\frac{\sin(n\omega t)}{n} \quad (4)$$

In which: $0 < \theta_1 < \theta_2 < \theta_3 < \pi/2$

$$H(n) = \frac{4V_{dc}}{n\pi}\left[\cos(n\theta_1)+\cos(n\theta_2)+\cos(n\theta_3)\right] \quad (5)$$

$$\begin{aligned}&\cos(\theta_1)+\cos(\theta_2)+\cos(\theta_3) = 3\pi/4\\ &\cos(5\theta_1)+\cos(5\theta_2)+\cos(5\theta_3) = 0\\ &\cos(7\theta_1)+\cos(7\theta_2)+\cos(7\theta_3) = 0\end{aligned} \quad (6)$$

From (6), the switching angles are $\theta_1 = 11.68^o$, $\theta_2 = 31.18^o$, and $\theta_3 = 58.58^o$, respectively. It is expected that the operation efficiency of the DSTATCOM using the step modulation is much higher than that of using high frequency switching techniques.

III. DSTATCOM Control Scheme

Figure 5 shows the studied system in the paper. A feedforward reactive power compensation scheme for the induction motor loads is employed for the DSTATCOM. Equ. (7) shows the three-phase complex power calculation of the induction motor loads, in which two-watt-meter method is used. The reactive power demand of the induction motor loads is obtained in (8). For real-time reactive power compensation of the induction motor loads during transient starting and steady-state operation, each arm of the DSTATCOM should continuously offer the reactive power compensation according to (9).

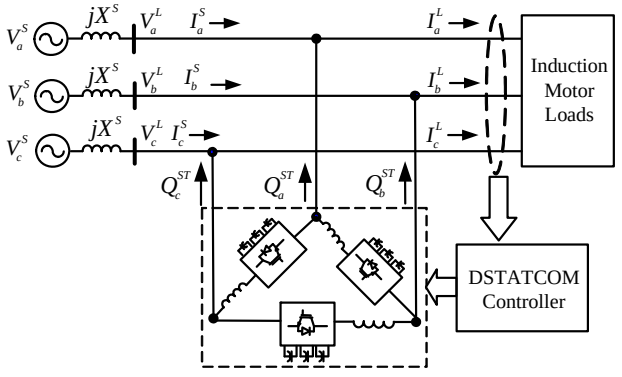

Fig. 5. The studied system

$$\begin{aligned}S^L_{3\phi} &= S^L_{ab} + S^L_{cb}\\ &= (\overline{V}^L_{ab})\cdot(\overline{I}^L_a)^* + (\overline{V}^L_{cb})\cdot(\overline{I}^L_c)^*\\ &= (P^L_{ab}+P^L_{cb}) + j(Q^L_{ab}+Q^L_{cb})\\ &= P^L_{3\phi} + jQ^L_{3\phi}\end{aligned} \quad (7)$$

$$Q^L_{3\phi} = Q^L_{ab} + Q^L_{cb} \quad (8)$$

$$\begin{bmatrix}Q^{ST*}_{ab}\\ Q^{ST*}_{bc}\\ Q^{ST*}_{ca}\end{bmatrix} = \frac{-1}{3}\begin{bmatrix}Q^L_{3\phi}\\ Q^L_{3\phi}\\ Q^L_{3\phi}\end{bmatrix} \quad (9)$$

Figure 6 shows the proposed block diagram of the DSTATCOM controller. First, the instantaneous line-to-line load bus voltages and line currents are detected to calculate the active and reactive powers absorbed by the induction motor loads according to (7)-(8). The needed reactive power commands of each DSTATCOM arm, Q^{ST*}_{ab}, Q^{ST*}_{bc}, and Q^{ST*}_{ca}, are calculated in real-time using (9). Three phase-locked loops (PLLs) generate synchronizing signals for the switching pattern generator. Three PI feedback controllers are employed to regulate the reactive power outputs of the three DSTATCOM arms independently, as shown in (10).

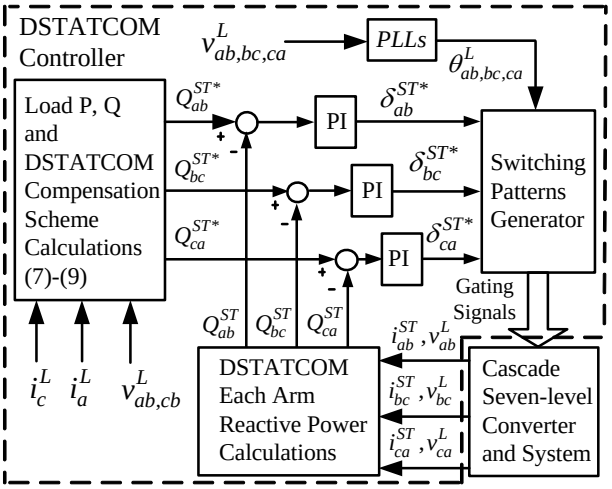

Fig. 6. DSTATCOM controller block diagram

$$\delta^{ST*}_{ab,bc,ca} = K_P\Delta Q^{ST}_{ab,bc,ca} + K_I\int \Delta Q^{ST}_{ab,bc,ca}\,dt \quad (10)$$

In which: $\Delta Q^{ST}_{ab,bc,ca} = Q^{ST*}_{ab,bc,ca} - Q^{ST}_{ab,bc,ca}$

Given the arm *a-b* for example, the reactive power output Q^{ST}_{ab} is measured and compared with the needed reactive power command Q^{ST*}_{ab}. The PI controller of the arm *a-b* receives the compared result and generates the needed power angle command δ^{ST*}_{ab}. Finally, use of the command δ^{ST*}_{ab} and the synchronizing signal generates the gating signals for the switching elements in the arm *a-b* according to Fig. 4.

IV. Simulation Result

A simulation system is developed in the Matlab/Simulink program for the preliminary functioning verification, as shown in Fig. 7. In the simulation, the starting responses of the induction motor with and without the DSTATCOM compensation are observed.

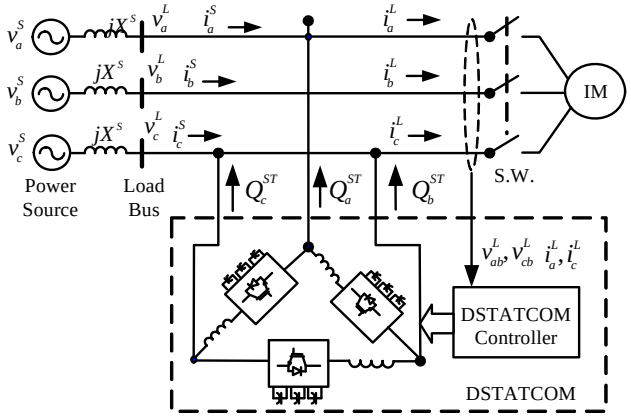

Fig.7. Simulation system setup

Case A. Without DSTATCOM Compensation

Figure 8(a) shows the starting current of the induction motor load, which contains a large amount of reactive power. The reactive power generates voltage sag on the load bus, as shown in Fig. 8(b). Fig. 8(c) shows the power demand of the induction motor during the starting. Obviously, the reactive power demand of the induction motor during the starting needs to be compensated for keeping satisfactory power quality.

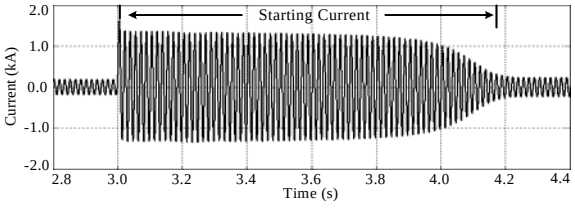

(*a*) phase-*a* source current

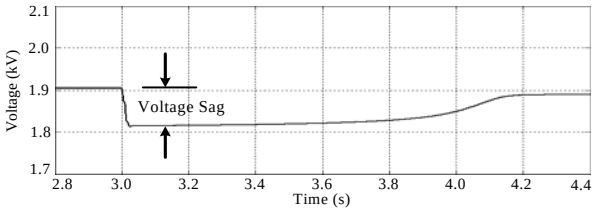

(*b*) phase-*a* Load voltage

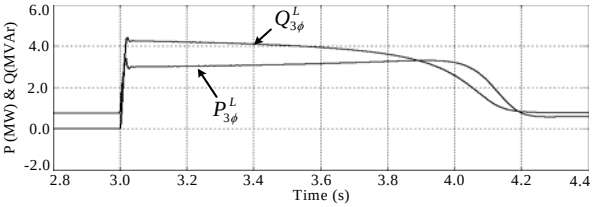

(*c*) load power demand

Fig. 8. Starting of induction motor without DSTATCOM compensation

Case B. With DSTATCOM compensation

Figure 9 shows the starting of the induction motor load with the real-time DSTATCOM compensation. Fig. 9(a) is the starting current of the induction motor. With the DSTATCOM compensation, the current from the power source is significantly reduced, as shown in Fig. 9(b). Figs. 9(c)-(d) show the internal voltage and current of the DSTATCOM arm *a*-*b*, respectively. The DSTATCOM response is very fast. The induction motor still needs reactive power for the starting, as shown in Fig. 9(e). With the DSTATCOM compensation, the reactive power from the power source is fully compensated, as shown in Fig. 9(f). The unity power factor correction is achieved.

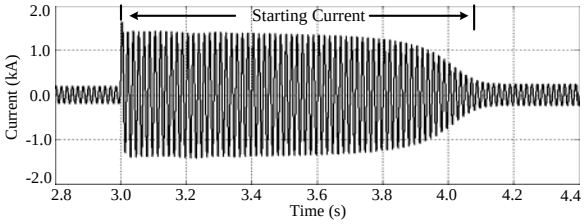

(*a*) phase-*a* load current

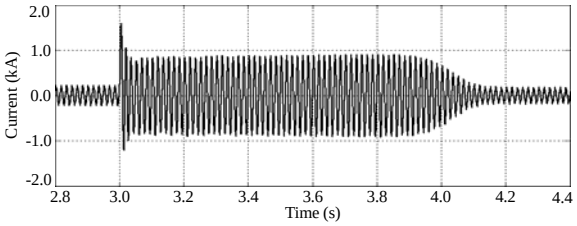

(*b*) phase-*a* source current

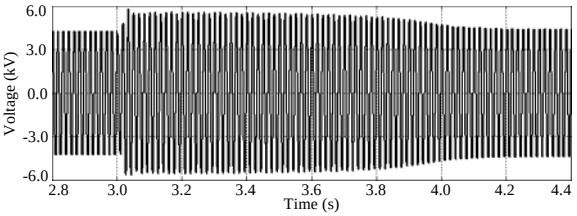

(*c*) arm *a*-*b* DSTATCOM internal voltage

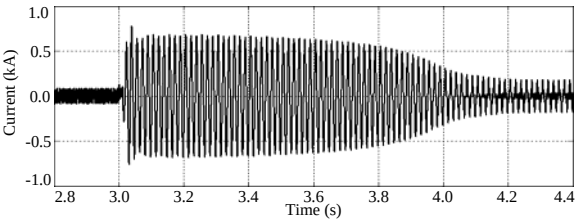

(*d*) arm *a*-*b* DSTATCOM internal current

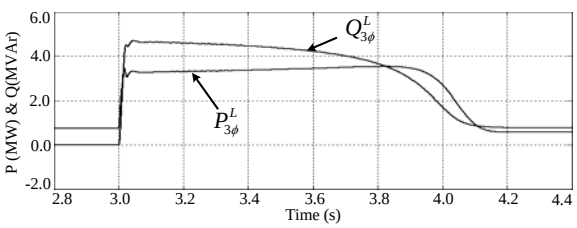

(*e*) load power demand

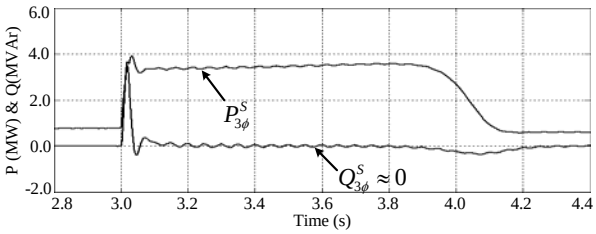

(*f*) power from the source

Fig. 9. Starting of induction motor with DSTATCOM compensation

Figure 10 shows a comparison of the induction motor performances with and without the DSTATCOM compensation. Fig. 10(a) is the load bus voltage responses. With the DSTATCOM compensation, the load bus voltage is kept at a stable operation. The rotor speed and induced torque responses of the induction motor during the starting can also be improved, as shown in Figs. 10(b)-(c).

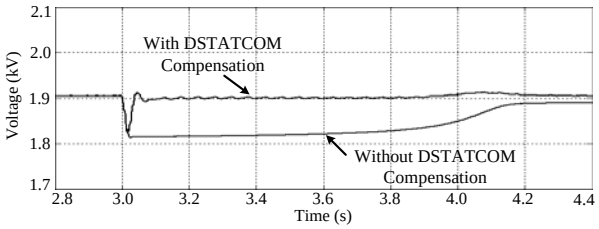

(*a*) Phase-*a* load bus voltage

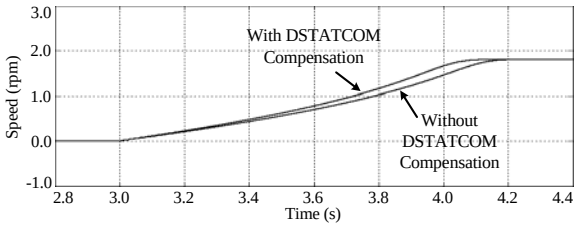

(*b*) rotor speed

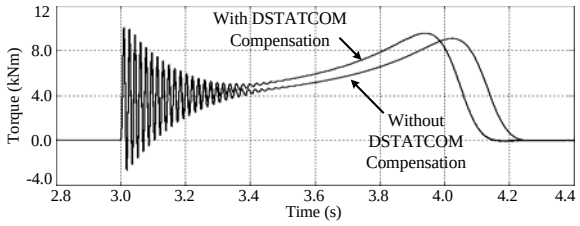

(*c*) induced torque

Fig. 10. Comparison of induction motor performance

V. Hardware Implementation

Figure 11 shows the block diagram of the DSTATCOM for hardware implementation. A three-phase induction motor is connected in parallel with the DSTATCOM as the tested load. The controller of the DSTATCOM is a multi-DSP-based system. A master-slaver controller architecture is used. The master controller in Fig. 11(a) is responsible for the load power detection and calculation of the compensation command.

The DSTATCOM main circuit is a transformerless, delta-connected structure. Three slaver controllers are used for reactive power regulations of the three DSTATCOM arms, independently. This arrangement enhances the reliability of the DSTATCOM operation in practical applications. Fig. 11(b) shows one main circuit and its slaver controller of the three DSTATCOM arms. The slaver controller receives the reactive power compensation command and calculates the needed switching angles. The gating signals are sent to switching elements in the FHB cells for reactive power regulation.

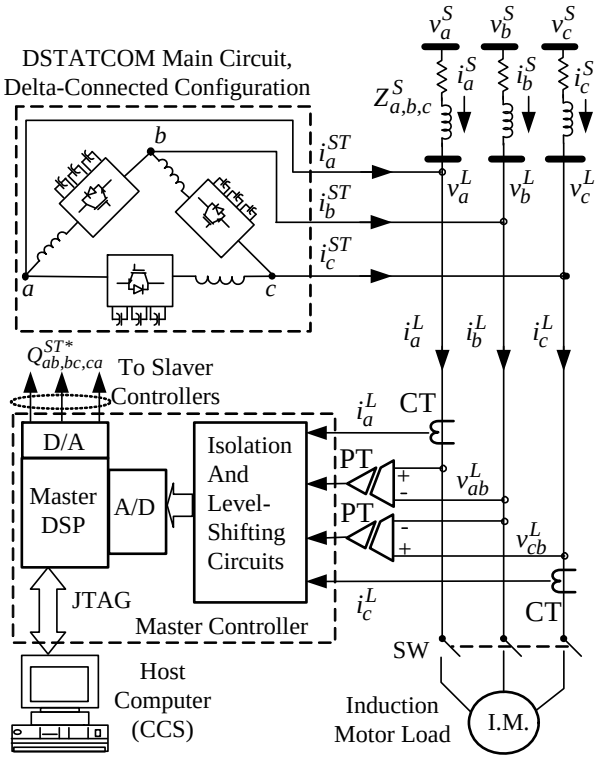

(a) DSTATCOM main circuit and master controller

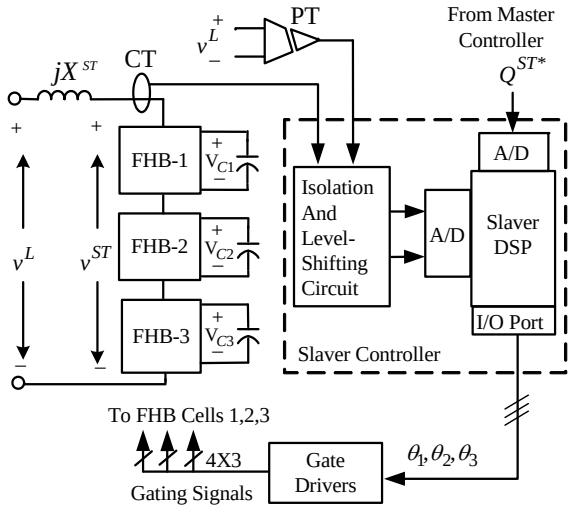

(b) one DSTATCOM arm and its slaver controller

Fig. 11. DSTATCOM main circuit and controller setup

Figures 12 and 13 show the hardware test results. Fig. 12 is the starting response of the induction motor with the DSTATCOM compensation. Figs. 12(a)-(b) record the starting current of the induction motor. The zoom-in waveform in Fig. 12(b) shows a demand of reactive power (lagging power factor). With the DSTATCOM compensation, the source current is quickly corrected to unity power factor, as shown in the zoom-in waveform in Fig. 12(d). It is observed that the amplitude of the source current in Fig. 12(c) is decreased. Fig. 12(e) shows the internal voltage responses of the three DSTATCOM arms. The internal voltages are boosted to offer the needed reactive power compensation according to (3). During the starting and steady-state operations of the induction motor load, the DSTATCOM continuously offers the needed reactive power for enhancement of the system operation. The DSTATCOM compensation is fast and satisfied.

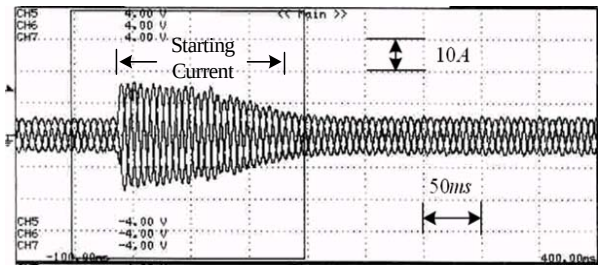

(a) three-phase load current response

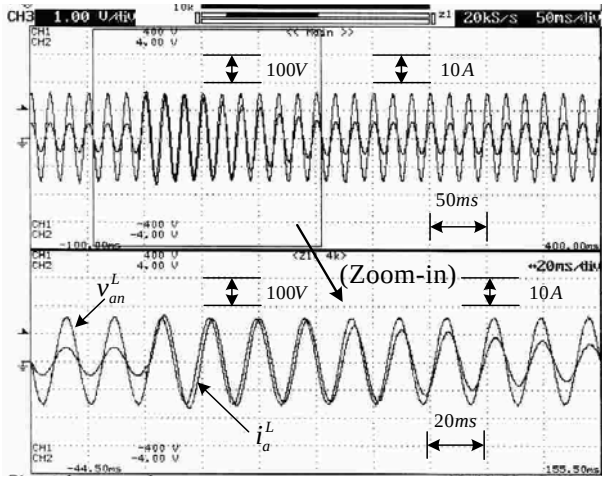

(b) phase-*a* load current i_a^L , and zoom-in waveform

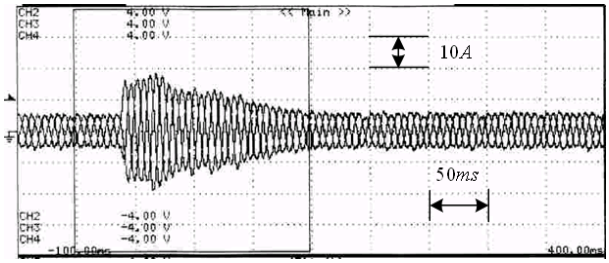

(c) three-phase source current response

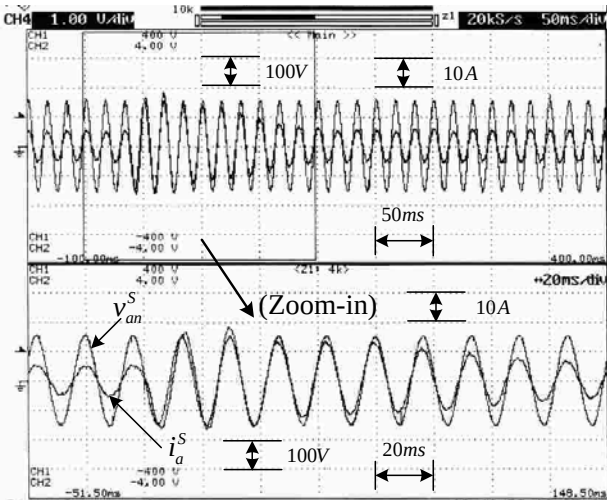

(d) phase-*a* source current i_a^S and zoom-in waveform

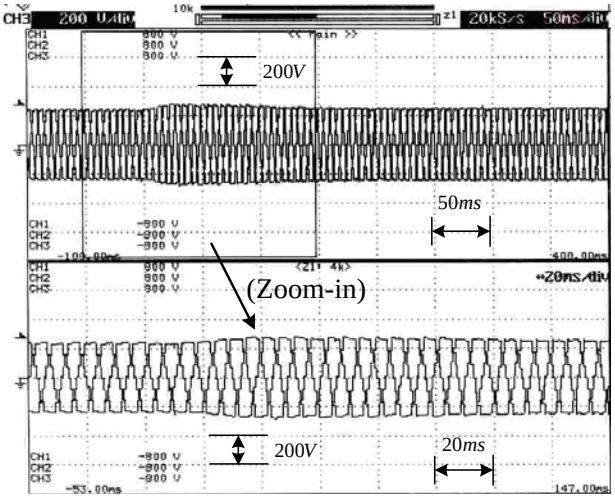

(e) DSTATCOM internal voltages response

Fig. 12. Acceleration of induction motor with DSTATCOM compensation

With the assistance of the real-time calculation ability in the DSP, the real-time three-phase active power $P_{3\phi}$ and reactive power $Q_{3\phi}$ to the load and from the source are obtained, as shown in Figs. 13(a)-(b). Fig. 13(a) records the reactive power demand during the starting. The reactive power from the power source is fully compensated very quickly, as shown in Fig. 13(b).

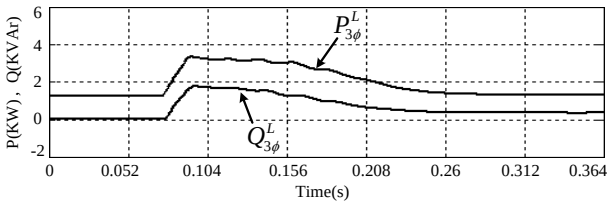

(*a*) power to the induction motor load

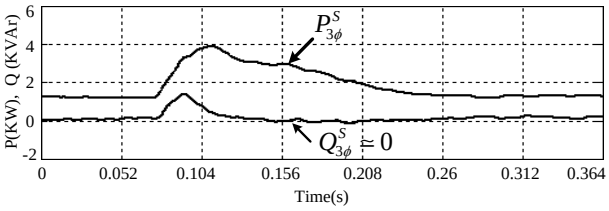

(b) power from the source

Fig. 13. Power flow with DSTATCOM compensation

Although the control scheme used in the DSTATCOM controller is very simple, the control effect is effective. The experimental results verify that the proposed DSTATCOM is suitable for real-time induction motor load compensation in industrial power systems.

VI. Conclusion

This paper has proposed the design and implementation of a multilevel cascade FHB converter-based DSTATCOM for real-time reactive power compensation and performance enhancement of induction motor loads in three-phase, three-wire industrial power distribution system. Compared to traditional SVC, the DSTATCOM needs less space demand for installation. Furthermore, its continuous regulation ability of reactive power is better than that of capacitor banks for power factor correction. Use of step modulation for the FHB cells in each DSTATCOM arm can obtains high efficiency operation in practical applications. A simple and effective feedforward compensation scheme is employed for the DSTATCOM, which makes the DSTATCOM more easily to be used in power industries. Experimental results show that the proposed DSTATCOM is very suitable for real-time performance enhancement of induction motor loads. It is hoped that the DSTATCOM can be widely employed in the future.

References

[1] M. H. J. Bollen, "The influence of motor reacceleration on voltage sags," *IEEE Transactions on Industry Applications*, Vol. 31, No. 4, pp. 667-674, 1995.

[2] J. C. Das, "Effects of momentary voltage dips on the operation of induction and synchronous motors," *IEEE Transactions on Industry Applications*, Vol. 26, No.4, pp. 711 -718, 1990.

[3] J. C. Gomez, M. M. Morcos, C. A. Reineri, and G. N. Campetelli, "Behavior of induction motor due to voltage sags and short interruptions," *IEEE Transactions on Power Delivery*, Vol. 17, No.2, pp. 434-440, 2002.

[4] B. Bhattacharyya, V. K. Gupta, and S. K. Goswami, "Application of DE & PSO algorithm for the placement of FACTS devices for economic operation of a power system," *WSEASTransactions on Power Systems*, Vol. 7, No. 4, pp. 209-216, 2012.

[5] S. P. Mangaiyarkarasi, and T. Sree Renga Raja, "A novel analytical study on voltage instability mitigation using multiple severity functions by optimal placement of SVC in N-2 contingency analysis using gravitational search algorithm," *WSEAS Transactions on Power Systems*, Vol. 9, pp. 408-417, 2014.

[6] S. V. Chandrakar, J. B. Helonde, R. M. Mohril, and V. K. Chandrakar, "Fuzzy based SVC with coordinated POD for damping of oscillations of power system," *WSEAS Transactions on Power Systems*, Vol. 5, No. 3, pp. 253-262, 2010.

[7] S. Teleke, T. Abdulahovic, T. Thiringer, and J. Svensson, "Dynamic performance comparison of synchronous condenser and SVC," *IEEE Transactions on Power Delivery*, Vol. 23, No. 3, pp. 1606-1612, 2008.

[8] J. Wang, C. Fu, and Y. Zhang, "SVC Control System Based on Instantaneous Reactive Power Theory and Fuzzy PID," *IEEE Transactions on Industrial Electronics*, Vol. 55, No. 4, pp. 1658-1665, 2008.

[9] T. J. E. Miller, *Reactive Power Control in Electric System*, John Wiley & Sons, New York, 1982.

[10] S. Y. Lee, C. J. Wu, and W. N. Chang, "A compact algorithm for three-phase three-wire system reactive power compensation and load balancing, " *Electric Power System Research*, Vol. 58, No. 2, pp.63-70, 2001.

[11] M. K. Mishra, and K. Karthikeyan, "A fast-acting DC-Link voltage controller for three-phase DSTATCOM to compensate AC and DC loads," *IEEE Transactions on Power Delivery*, Vol. 24, No. 4, pp. 2291-2299, 2009.

[12] B. Singh, and J. Solanki, "A comparison of control algorithms for DSTATCOM," *IEEE Transactions on Industrial Electronics*, Vol. 56, No. 7, pp. 2738-2745, 2009.

[13] L. Gyugyi, "Dynamic compensation of AC transmission lines by solid-state synchronous voltage sources," *IEEE Transactions on Power Delivery*, Vol. 9, No. 2, pp. 904-911, 1994.

[14] H. Akagi, "Classification, terminology, and application of the modular multilevel cascade converter (MMCC)," *IEEE Transactions on Power Electronics*, Vol. 26, No. 11, pp. 3119-3130, 2011.

[15] C. K. Lee, J. S. K. Leung, S. Y. R. Hui, and H. S. H. Chung, "Circuit-level comparison of STATCOM technologies," *IEEE Transactions on Power Electronics*, Vol. 18, No. 4, pp. 1084-1092, 2003.

[16] J. Rodriguez, J. S. Lai, and F. Z. Peng, "Multilevel inverters: a survey of topologies, controls, and applications," *IEEE Transactions on Industrial Electronics*, Vol. 49, No. 4, pp. 724-73, 2002

[17] C. T. Lee, B. S. Wang, S. W. Chen, S. F. Chou, J. L. Huang, C. P. Tai, H. Akagi, and Barbosa, P., "Average power balancing control of a STATCOM based on the cascaded H-bridge PWM converter with star configuration," *IEEE Transactions on Industry Applications*, Vol. 50, No. 6, pp. 3893-3901, 2014.

[18] M. Hagiwara, R. Maeda, and H. Akagi, "Negative-sequence reactive-power control by a PWM STATCOM based on a modular multilevel cascade converter (MMCC-SDBC)," *IEEE Transactions on Industry Applications*, Vol. 48, No. 2, pp. 720-729, 2012.

[19] F. Z. Peng, J. S. Lai, J. W. McKeever, and J. VanCoevering, "A multilevel voltage-source inverter with separate DC sources for static VAr generation," *IEEE Transactions on Industry Applications*, Vol. 32, No. 5, pp. 1130-1138, 1996.

[20] S. Sirisukprasert, J. S. Lai, and T. H. Liu, "Optimum harmonic reduction with a wide range of modulation indexes for multilevel converters," *IEEE Transactions on Industrial Electronics*, Vol. 49, No. 4, pp. 875-881, 2002.

[21] Y. Liu, H. Hong, and A. Q. Huang, "Real-time calculation of switching angles minimizing THD for multilevel inverters with step modulation," *IEEE Transactions on Industrial Electronics*, Vol. 56, No. 2, pp. 285-293, 2009.